Published in final edited form as:

Oncogene. 2017 May 18; 36(20): 2846–2856. doi:10.1038/onc.2016.436.

COOPERATION AMONG HETEROGENEOUS PROSTATE CANCER CELLS IN THE BONE METASTATIC NICHE

Kristina Shahriari[1], **Fei Shen**[1], **Asurayya Worrede-Mahdi**[1], **Qingxin Liu**[1,†], **Yulan Gong**[2], **Fernando U. Garcia**[2,4], and **Alessandro Fatatis**[1,2,3]

[1]Department of Pharmacology and Physiology, Drexel University College of Medicine, Philadelphia, PA

[2]Department of Pathology and Laboratory Medicine, Drexel University College of Medicine, Philadelphia, PA

[3]Program in Prostate Cancer, Sidney Kimmel Cancer Center, Thomas Jefferson University, Philadelphia, PA

[4]Cancer Treatment Centers of America, Eastern Regional Medical Center, Philadelphia PA

Abstract

The growth of disseminated tumor cells (DTCs) into metastatic lesions depends on the establishment of a favorable microenvironment in the stroma of the target organs. Here we show that mice treated with anakinra, an antagonist of the IL-1β receptor (IL-1R), or harboring a targeted deletion of IL-1R are significantly less prone to develop bone tumors when inoculated in the arterial circulation with human prostate cancer (PCa) cells expressing IL-1β. Interestingly, human mesenchymal stem cells (hMSCs) exposed *in vitro* to medium conditioned by IL-1β-expressing cancer cells responded by up regulating S100A4, a marker of cancer-associated fibroblasts (CAFs), and this effect was blocked by anakinra. Analogously, the stroma adjacent to skeletal metastases generated in mice by IL-1β-expressing cancer cells showed a dramatic increase in S100A4, COX-2 and the alteration of thirty tumor-related genes as measured by Nanostring analysis. These effects were not observed in the stroma associated to the rare and much smaller metastases generated by the same cells in IL-1R knockout animals, confirming that tumor-secreted IL-1β generates skeletal CAFs and conditions the surrounding bone microenvironment. In skeletal lesions from patients with metastatic PCa, histological and molecular analyses revealed that IL-1β is highly expressed in cancer cells in which the androgen receptor (AR) is not detected (AR−) whereas this cytokine is uniformly absent in the AR-positive (AR+) metastatic cells. The stroma conditioned by IL-1β-expressing cancer cells served as a supportive niche also for coexisting IL-1β-lacking cancer cells, which are otherwise unable to generate tumors after independently

Corresponding Author: Alessandro Fatatis, M.D., Ph.D., Department of Pharmacology and Physiology, Drexel University College of Medicine, 245 N. 15th Street, NCB 8211. Philadelphia, PA 19102, Phone (215) 762 8534 - Fax (215) 762 2299.
†Current address: Department of Systems Biology, The University of Texas MD Anderson Cancer Center, Houston TX.

Supplementary Information accompanies the paper on the Oncogene website (http://www.nature.com/onc).

The authors declare no conflict of interest.

seeding the skeleton of mice. This niche is established very early following tumor seeding and hints to a role of IL-1β in promoting early colonization of PCa at the skeletal level.

Keywords

Prostate Cancer; Metastasis; Heterogeneity; Microenvironment; IL-1R

INTRODUCTION

During the initial settlement that follows extravasation into target organs, cancer cells may benefit from existing supportive niches or must condition the surrounding stroma in their favor. The second event involves the recruitment of bystander cells in the normal parenchyma and the establishment of a habitat prone to tumor growth. It is widely recognized that these tumor-initiating abilities are not shared by all cancer cells but rather are a prerogative of a restricted fraction of malignant phenotypes. On a quest for signaling molecules capable of conditioning the bone microenvironment in support of metastatic growth, we focus on IL-1β, a cytokine that has been associated with tumor-promoting effects [1,2,3], but with only circumstantial implication in metastasis [4]. In a previous study we used DNA microarray-based screening and identified IL-1β as an over-expressed gene conferring metastatic behavior to the human PC3-ML cells tested inanimal models [5]. Building on this initial evidence, in this study we used the same animal model to show a clear impairment of skeletal tumor growth upon systemic administration of an IL-1R inhibitor. Furthermore, the use of transgenic mice knockout for IL-1R provided additional support to the idea that tumor-derived IL-1β is necessary for conditioning the bone stroma into a metastasis-receptive niche. In addition, *in vitro* studies and the harvesting of tumor-associated bone stroma in mice suggested a local development of CAFs from MSCs and alteration of thirty tumor-associated genes – including COX-2 – both resulting from signaling through IL-1R. To correlate this pre-clinical evidence with human pathology, we tested skeletal metastases from ten different PCa patients for IL-1β expression and found the considerable fraction of cancer cells with undetectable AR also lacking IL-1β. Notably, the inverse relationship between AR and IL-1β expression we observed in human metastatic PCa cells corresponds, in animal models, to a bone-metastatic behavior restricted exclusively to the AR–/IL-1β-expressing phenotype of PC3-ML cells. Finally, the metastatic niche generated by PC3-ML also supports the growth of the PCa malignant phenotypes that lack IL-1β and consistently fail to survive after disseminating to the skeleton. Based on these findings, we propose that PCa cells secreting IL-1β are instrumental in priming the bone metastatic niche for initial colonization.

RESULTS

Antagonism of IL-1β signaling impairs metastasis

We grafted human cancer cells directly into the arterial circulation of SCID mice via the left cardiac ventricle, thus generating CTCs that disseminate systemically in an unbiased fashion and closely reproduce the spreading of solid tumors in human patients [6]. Stably fluorescent PC3-ML cells, a sub-line of the parental PC3 [7] that lacks AR, highly expresses IL-1β [5] and

shows metastatic tropism for the skeleton [8], were inoculated in mice pretreated for one day with either vehicle or the IL-1R antagonist anakinra [9]; these treatments continued daily for two weeks until sacrifice. Animals treated with anakinra showed a significant and dose-dependent reduction in tumor burden (Figure 1a,b) as compared to controls. Notably, the impairment in tumor growth observed in animals treated with 40 mg/kg of anakinra equaled the results we obtained in a previous study by silencing IL-1β expression *via* RNA interference [5].

IL-1β recruits the bone stroma to support tumor growth in the skeleton

Tumor-derived IL-1β could act in a paracrine fashion on the surrounding bone stroma, which might then reciprocate by providing crucial trophic support for tumor growth. To specifically address this issue, we generated IL-1R knockout SCID mice and inoculated them and their IL-1R-wild-type littermates with PC3-ML cells, sacrificing after two weeks. The absence of IL-1R in the bone stroma harboring the disseminated cancer cells in knockout animals completely prevented tumor growth in 50% of these mice (Figure 1c) and dramatically reduced the size of the skeletal tumors detected in the remaining animals (Figure 1d,e).

Tumor-derived IL-1β converts bone hMSC into CAFs in vitro and induces expression of CAFs markers and bone stromal alterations in vivo

Having thus identified the stroma as a key driver of IL-1β-mediated metastasis, we sought to further explore its activity during skeletal metastatic progression. We exposed hMSCs *in vitro* for one week to IL-1β peptide (25 pg/mL) or CM from PC3-ML cells, then examined for morphological and biochemical markers indicating their conversion to CAFs [10]. CAFs have a well-established role in primary tumors [11,12] and are widely thought to act similarly at secondary sites. We found that hMSCs responded to IL-1β by formation of elongated actin stress fibers, suggestive of a transition into CAFs [13]; a similar change in morphology was generated by CM from PC3-ML cells, which are known to secrete IL-1β [5]. In either case, the effect observed was abrogated by inclusion of anakinra in the culture medium (Figure 2a). Consistent with this finding, the expression of the CAF-marker S100A4 (also known as FSP1) increased in hMSCs exposed to either IL-1β peptide or CM from PC3-ML cells, an effect which again was blocked by anakinra (Figure 2b). In light of these *in vitro* findings, we proceeded to determine whether the stroma surrounding skeletal metastases in our animal model responded to tumor-secreted IL- 1β in a similar fashion. Bone stroma immediately adjacent to and some distance away from tumors generated by PC3-ML cells was harvested by LCM from IL-1R wild-type mice (Figure 2c, left); in the same animals, stroma from bones which did not harbor any tumors was also collected (Figure 2c, middle); as were analogous samples from IL-1R knockout mice (Figure 2c, right). These tissues were tested for S100A4 and COX-2 expression, as both molecules are known to be induced in stromal cells by exposure to IL-1β [514], and S100A4 expression would indicate the development of CAFs in the metastatic niche [15]. We detected a strong induction of both markers in the bone stroma of wild-type animals immediately adjacent to the skeletal tumors relative to the normal tissue. This effect appeared spatially delimited: stroma located some distance from tumors was only minimally affected, likely due to the concentration gradient of IL-1β secreted by the cancer cells. Further, in IL-1R knockout animals the expression of

stromal S100A4 and COX-2 was totally unaffected by the presence of tumors, confirming the causal role of IL-1 signaling in this process (Figure 2d).

IL-1β affects the expression of tumor-related genes in the bone stroma

The growth-permissive niche generated by IL-1β likely involves alterations in local concentrations of molecular mediators produced by cells either naturally inhabiting the bone stroma or migrating to the tumor-colonized tissue microenvironment. With the intent of identify specific genes altered by IL-1β signaling in tumor-associated bone stromal cells, we interrogated the same LCM mouse tissue specimens analyzed above for S100A4 and COX-2 expression by using Nanostring technology and an nCounter panel of 750 genes with established relevance in adaptive, humoral, and innate immune response as well as inflammation. We detected 30 genes for which expression was significantly altered two folds or more by the presence of prostate cancer cells as compared to bone stroma either free of tumors or harvested from IL-1R KO animals (Table 1).

Correlation between IL-1β expression and AR status in human skeletal metastases

In order to translate our results using animal models to human metastatic disease, we investigated IL-1β expression in archival bone biopsies obtained from ten patients in two different clinical cohorts and with documented post-ADT metastatic CRPC. In previous studies, we had observed a negative correlation between PSA immunostaining (as a measure of AR transcriptional activity) and IL-1β expression in bone metastases from a different cohort of patients [5]. In this new group of patients, we found that the AR− prostate cancer cells showed high IL-1β expression, while the AR+ cells tested completely negative for this cytokine. Interestingly, these specimens revealed remarkable variability of AR staining within individual lesions (Figure 3a, arrows), while in some areas the AR could be detected in only a minority of cancer cells (Figure 3a, dotted line). Overall, more than 30% of cancer cells identified by morphological and histopathological criteria in these ten patients did not stain for AR (Figure 3b). Furthermore, dual immunofluorescence staining with an AR and a pan-cytokeratin antibody [16] indicated that the cancer cells identified in these metastatic lesions, both with and without AR expression, were of epithelial origin, as can be seen at both primary (Figure 3c) and bone metastatic sites (Figure 3d). To provide molecular validation of these findings, we employed LCM to harvest tumor and stromal tissues (Supplemental figure 1) from two of the same bone-metastasis specimens examined by IHC staining (patients 2 and 4) and analyzed them by qRT-PCR. The prostatic origin of both AR+ and AR− tumor cells was conclusively established by the equivalent levels of mRNA for prostein (also known as SLC45A3 or P501S), which is highly restricted to both normal and malignant prostate cells and is routinely used for the diagnosis of metastatic lesions [17-19] (Figure 3e). The AR status indicated by IHC staining was confirmed at the transcriptional level (Figure 3f). Notably, AR− cancer cells did not express molecular neuroendocrine (NE) markers such as synaptophysin or chromogranin A [20,21] (Supplemental table 1), in contrast to a lung metastasis from another patient that stained negative for AR expression but expressed NE markers, as is frequently observed in visceral lesions typical of advanced PCa. (Supplemental figure 2 and Supplemental table 1).

In comparison to AR– cancer cells, bone stroma expressed significantly lower levels of IL-1β transcript (Figure 3g). This indicates that PCa cells play a dominant role in dictating the local levels of IL-1β during colonization of the skeleton, in contrast to what has been previously proposed by others using subdermal implant of bioengineered scaffolds [22].

The bone stroma conditioned by metastatic cells supports also the colonization of cells with indolent metastatic behavior

We surmised that PC3-ML cells could also be supportive of indolent cancer cells that are incapable of independently generating the molecular crosstalk necessary to support survival and therefore fail to colonize the bone. To test this hypothesis and in light of the pro-metastatic role of IL-1β revealed by our study thus far, we first assessed the expression of this cytokine in additional human PCa cells either lacking (DU-145) or expressing (LNCaP, VCaP, and 22Rv1) the AR. We found all cell types to be negative for IL-1β (Figure 4a) and unable to metastasize in our animal model, despite successfully arriving to the skeleton via the arterial circulation and homing as DTCs. This is consistent with our previous work with DU-145 cells [85], with the lack of published studies with LNCaP and VCaP cells in pre-clinical models of bone metastasis, and only two existing reports for 22Rv1 cells [2324], the results of which could not be reproduced in our hands. We then generated PC3-ML cells stably expressing both the fluorescent protein mCherry and RedLuc, to be paired with the various non-metastatic cell lines, which were engineered to express GFP and Luc2. Co-inoculation experiments were then conducted to ascertain whether metastatic PC3-ML cells could support colonization of the skeleton by independently non-metastatic cells in mice (Figure 4b). We found that this was indeed the case, as mixed tumors could be detected by bioluminescent imaging (BLI) and multispectral fluorescence microscopy for all cell combinations (Figure 4c,d). At 4 weeks, animals in each study were found to harbor skeletal tumors comprised solely of PC3-ML cells as well as mixed tumors located in upper limbs, lower limbs and spine.

Cooperation between cancer cells starts early after seeding the bone marrow

Next, we sought to determine whether the cooperation among cancer cells revealed by the experiments described above is an early event, or one that takes time to be established. To dissect the earliest stages of metastasis, we examined the bones of animals sacrificed 24 hours after intracardiac co-inoculation of PC3-ML cells and a non-metastatic cell line. These animals revealed that the presence of PC3-ML cells led to a significant increase in the number of non-metastatic 22Rv1 and VCaP cells found in the skeleton, compared to unaccompanied inoculation of these cells (Figure 5a,b). These findings denote a pro-metastatic role for PC3-ML cells that begins very rapidly after the initial lodging of cancer cells in the skeleton and leads to critical changes in the bone microenvironment during the first 24 hours of seeding. While these data might hint to a role for IL-1β in the bone-metastatic niche, we had yet to understand the trajectory of the crucial IL-1 signaling. To this end, we assayed the various PCa cell lines used in this study for expression of the IL-1R in order to determine their potential receptivity to paracrine IL-1β signaling, and found the receptor present in each (Figure 5c). However, exposure to IL-1β peptide *in vitro* revealed a varying profile of signal transduction among two AR+ PCa cell lines that benefited equally from PC3-ML cells when colonizing the bone, suggesting that paracrine stimulation of

IL-1R is unlike to be primarily responsible for the metastatic cell cooperation we observed (Figure 5d). On the other hand, hMSCs, which are an abundant component of the bone stroma, when similarly exposed to IL-1β exhibited a rapid and sustained signaling response, indicating definite susceptibility to this cytokine (Figure 5e). Interestingly, we showed the cooperative arrival effect appear to be specific to the bone microenvironment, as no difference in seeding was observed in the lungs of the animals described above (Figure 5f,g).

Exogenous expression of IL-1β is sufficient to induce a metastatic phenotype that cooperates with indolent cancer cells

Here we sought to strengthen the findings described above by testing the role of IL-1β in supporting cells lacking this cytokine and unable to independently metastasize. To this end, we generated non-metastatic DU-145 cell line engineered to stably express high levels of IL-1β (Figure 6a), which we have previously shown to impart them with *de novo* metastatic ability [5]. Notably, these cells would – at least in part - mimic the AR −/ IL-1β-expressing phenotype of PC3-ML cells and be consistent with the inverse correlation between AR and IL-1β that we had observed in skeletal metastases from PCa patients. These newly generated DU-145 cells were labeled with mCherry/Red Luc and co-injected with GFP/Luc2-labeled VCaP cells, and the mice sacrificed after either 24 hours or three weeks later. Upon examination of their femora and tibiae, which we routinely inspect to assess cancer cell seeding [25], we found a significant increase in arrival of VCaP cells (Figure 6b), and generation of mixed tumors (Figure 6c) relative to their solitary inoculation.

DISCUSSION

Given our previous findings regarding the importance of IL-1β expression to the bone metastatic behavior of human prostate cancer cells [5], we sought to determine whether this cytokine exerts a functional role in promoting metastasis through experimental interference with its signaling. To strictly address the clinical scenario of advanced prostate cancer in a pre-clinical setting, we focused on late stages of the metastatic process: bone colonization and progression into macroscopic skeletal lesions. Our studies provide first and convincing evidence that interfering with IL-1R activation using an FDA-approved drug such as anakinra [26] impairs tumor growth at the skeletal level in a clinically-relevant animal model of metastatic PCa. Significantly, experiments with transgenic knockout mice showed that the aggressive bone-metastatic behavior of PC3-ML cells was severely undermined by the absence of IL-1R expression by the tissue hosting the cancer cells. This hints to an essential role for IL-1β secreted by PCa cells in recruiting cellular components of the bone microenvironment to establish a tumor-receptive metastatic niche. Additional experiments pointed to hMSC as a cell types likely involved in this tumor-stroma cross talk, as these cells converted into CAFs *in vitro* when exposed to CM from PC3-ML cells and we detected elevated markers of this conversion such as S100A4 and COX-2 in the bone stroma closely associated to tumors. The fact that both markers have been also mechanistically implicated in the tumor-promoting role of CAFs [14,27] provides additional support to the idea of a bone stroma reciprocating to PCa-mediated IL-1β signaling by promoting metastatic colonization.

Furthermore, our gene profiling studies identify alterations in mediators of tumor growth and progression affecting the bone stroma within the metastatic niche. In addition to confirming the up-regulation of *COX-2* previously detected by qRT-PCR, we found that the up-regulation of Integrins α1, β2 and β4, Osteopontin, Tumor Necrosis Factor (TNF) 13 (TNF13 or BAFF) and TNF receptor 17 both corroborates earlier studies by others [28-30] and delineates a profile of pro-tumorigenic genes regulated by IL-1β secreted from metastasis-initiating cells. Equally compelling is the 7-fold down-regulation of interleukin-24 (IL-24), a cytokine with a pleiotropic tumor-suppressing role that involves decreasing stemness of human prostate cancer cells [31], which supports the need for lessening its expression during tumor colonization of the metastatic niche. On the same line, down-regulation of two initiating components of the Complement cascade (C1r and C1s) and of Manna-binding lectin serine peptidase 2 (Masp2) [32] hints to an impairment of the innate immune-response, which has been proposed to control tumor growth *via* several types of immune cells including NK cells [33,34]. As NK cells are normally present in immune-compromised SCID mice, which were used in our study, these results delineate a conceivable scenario in which tumor-derived IL-1β mitigates the killing of cancer cells by innate immune response in the bone microenvironment.

By examining human specimens from metastatic patients we revealed an inverse correlation between IL-1β and AR expression in PCa cells. Molecular analyses conclusively show that approximately one-third of cancer cells in skeletal lesions do not express AR and, in contrast to AR+ cancer cells, are highly positive to IL-1β. Remarkably, these AR− phenotypes do not express NE markers [35], differing from visceral metastases typical of the advanced disease [3637] and most likely could not be traced either to a primary small-cell carcinoma or to AR+ PCa cells transitioning into an NE phenotype [3835]. Even in light of the recognized dynamic regulation of both AR [39,40] and IL-1β expression [41], our study reveal a bone-metastatic environment in which PCa cells may display either a stable or fluctuating AR−/IL-1β+ phenotypes but are – at any given time – numerically relevant and likely capable of coercing the stroma into a niche favorable to tumor growth by secreting IL-1β.

The AR−/IL-1β+ phenotypes detected in patients are mimicked by PC3-ML cells, which were found capable of supporting skeletal colonization and growth of both AR− (DU-145) and AR+ (LNCaP, VCaP and 22Rv1) PCa cells that lack IL-1β and fail to metastasize independently. The heterogeneous tumors generated in our animal models are particularly compelling as they reproduce the scenario observed in patients and overall reflect the widely-reported genetic, hormonal, and likely functional heterogeneity of cancer cells in human metastases [4243]. A highly speculative but yet intriguing concept is that DU-145 cells could exemplify an AR− PCa phenotype not expressing IL-1β and thus lacking bone-tropism, as shown by their derivation from a human brain metastasis [44]. However, the possibility of rare subpopulations of AR− PCa cells lacking IL-1β and coexisting with AR−/IL-1β+ cancer cells in PCa bone metastases is also plausible.

Nonetheless, the exogenous expression of IL-1β in DU-145 cells was sufficient to confer bone-metastatic behavior [5] as well as the ability to support the initial colonization of non-metastatic PCa cells after arrival to the skeleton.

In conclusion, our study provides pre-clinical evidence that the conditioning of the bone stroma by tumor-derived IL-1β spawns a niche permissive to the growth of PCa cells, outlines IL-1β as orchestrating heterotypic cell-cell communications and reveals a complex skeletal metastatic environment, in line with similar cellular dynamics observed in primary tumorigenesis [45]. Collectively, these results hint to a conceivable metastasis-promoting role for AR− /IL-1β+ PCa cells, describe and characterize a previously unknown functional heterogeneity in metastatic prostate cancer and provide a strong incentive for clinical testing of pharmacological agents targeting both IL-1β signaling and stromal reciprocation, either as a standalone approach or in combination with the current standard of care.

MATERIALS AND METHODS

Cell lines and culture

DU-145, 22Rv1, LNCaP, and VCaP human prostate cancer cell lines were purchased from ATCC; the PC3-ML cell line was derived from the parental PC-3 cell line as previously described [7]. All cell lines were cultured at 37°C and 5% CO_2, authenticated by short tandem repeat profiling by IDEXX Radil and/or DDC Medical and discarded ten passages after thawing. We used Dulbecco's Modified Eagle Medium (DU-145, VCaP, and PC3-ML) or RPMI-1460 (22Rv1 and LNCaP) containing 10% fetal bovine serum and 0.1% gentamicin. Bone marrow-derived human MSCs (Lonza) were used between passage 5 and 8 and cultured in α-MEM supplemented with 10% FBS, 1 ng/ml bFGF (R&D), and 0.1% gentamicin. Conditioned media experiments were performed as previously described [5].

Viral vectors for stable gene expression

Stable expression of the fluorescent markers eGFP and mCherry, the luciferase enzymes Red Firefly Luciferase and Luc2, and the cytokine IL-1β were achieved through lentiviral transduction with the following constructs: pLenti CMV GFP Blast (659-1), pLenti CMV Blast empty (w263-1), pLenti CMV Puro DEST (w118-1), and pENTR1A no ccDB (w48-1) were gifts from Eric Campeau (Addgene plasmids # 17445, 17486, 17452, and 17398). pLenti CMV mCherry Blast was produced by subcloning the mCherry gene from pmCherry-N1 (Clontech, Mountain View, CA, USA) into the BamHI and XbaI sites of pLenti CMV Blast empty. pLenti CMV Red Luc Puro and pLenti CMV Luc2 Puro were produced by first subcloning the Red Firefly Luciferase gene from pMCS-Red Firefly Luc (Thermo Fisher Scientific, Waltham, MA, USA) or the Luc2 gene from pGL4.51[luc2/CMV/Neo] (Clontech) into the BamHI and XhoI sites of pENTR1A no ccDB; pLenti CMV IL-1β Puro was produced by initially shuttling human IL-1β cDNA (NM_000576) into the SalI and BamHI sites of pENTRA1A no ccdB. Each of these inserts was then transferred via Gateway LR Clonase II (Invitrogen) into pLenti CMV Puro DEST.

SDS-PAGE and Western Blotting

Western Blotting analysis was performed as previously described [46]. Primary antibodies were: S100A4 at 1:500 (ab27957, Abcam); IL-1β at 1:250 (SC-7884, Santa Cruz Biotechnology); Actin at 1:3000 (A-2066, Sigma-Aldrich); phospho-IκBα Ser32 at 1:500 (#2859), IκBα at 1:500 (#4814), phospho-NF-κB p65 Ser536 at 1:1000 (#3033), NF-κB

p65 at 1:1000 (#8242), and GAPDH at 1:5000 (#5174), all from Cell Signaling Technology. HRP-conjugated secondary antibodies were used at 3.33 ng/ml.

Immunofluorescence

Formalin-Fixed Paraffin-Embedded (FFPE) sections of primary PCa and bone metastases were obtained from the archives of the Department of Pathology at Drexel University College of Medicine and stained using a FITC-conjugated Pan-Cytokeratin antibody (clone C-11) and an antibody against the N-20 region of the human Androgen Receptor (Dr. Karen Knudsen, Sidney Kimmel Cancer Center at Thomas Jefferson University) and then imaged using an Axio Scope A1 microscope (Zeiss) paired with the Nuance Multispectral Imaging System (PerkinElmer). hMSCs cells were treated, fixed in 4% paraformaldehyde and stained with Anti-Actin, α-Smooth Muscle - Cy3™ (clone 1A4). Samples were imaged with an LSM 5 Exciter Axio Imager Z1m confocal microscope (Zeiss).

Animal studies and statistics

Male C.B17-SC mice (Taconic) at six to eight weeks of age were anesthetized with ketamine (80 mg/kg) and xylazine (10 mg/kg) prior being inoculated with cancer cells *via* the left cardiac ventricle [47]. Animals that upon being imaged one week after inoculation showed a diffuse bioluminescence signal in the chest area were deemed misinjected and therefore excluded from the study. For anakinra experiments, animals received subcutaneous injections of vehicle (PBS) or anakinra (Swedish Orphan Biovitrum) at the indicated doses. All experiments were performed in accordance with NIH guidelines for the humane use of animals. The Drexel University College of Medicine Institutional Animal Care and Use Committee approved all protocols involving the use of animals.

For this study we used descriptive statistics. A pre-specified effect size was not selected prior to conducting the experiments. After intracardiac injection, the experimenter distributed each animal in unlabeled cages. Each cage was randomly assigned to different treatment groups by a second experimenter. In the assessment of the outcome for in vivo imaging of longitudinal studies, the experimenter was not blinded but was assisted by the IVIS Living Image Software in calculating the site and extent of photon emission as indications of tumor localization and growth, respectively. For the detection and enumeration of single tumor cells, the experimenter was not blinded but was assisted by the Nuance FX multiplex imaging software. A fluorescence image was acquired for each tissue section analyzed; the identification and enumeration of single cells was obtained by three different experimenters, including the Principal Investigator, and occasional discrepancies reconciled prior to compiling the final data. One-way Anova was used to compare multiple experimental groups. Student's *t*-test with Welch's correction (Prism 5.0) was used to compare two experimental groups assuming no equal variance.

Generation of IL-1R SCID mice

IL-1R SCID mice were generated by crossing CB17-SC RF mice with transgenic animals knockout for *IL-1R1* (OMIM 147810, from Dr. Nancy McNamara, UCSF). These animals were then genotyped for the $Prkdc^{scid}$ mutation by PCR using the forward primer 5'-GGAAAAGAATTGGTATCCAC-3' and reverse 5'-AGTTATAACAGCTGGGTTGGC-3';

the product was digested with AluI resulting in fragments of 68 and 11 bp (wild-type) and 38, 28, and 11 bp (SCID). IL-1R status was determined by multiplex PCR using the following primers: IL-1R WT Fwd- 5'-CCACATATTCTCCATCACTCTGCTGGTA-3', IL-1R WT Rev- 5'-TTTCGAATCTCAGTTGTCAAGTGTGTCCC-3', IL-1R KO Fwd- 5'-CTGAATGAACTGCAGGACGA-3', IL-1R KO Rev- 5'-ATACTTTCTCGGCAGGAGCA-3', and resulting in amplification of fragments of 350 base pairs (wild-type allele) and 172 base pairs (knockout) (Supplemental Figure 3). Once animals homozygous for *Prkdc*^{scid} and heterozygous for IL-1R were obtained the colony was maintained through intercross of IL-1R heterozygotes, with six- to eight-week-old male wild type and knockout littermates used for the experiments.

In vivo bioluminescence imaging

Prior to each weekly imaging session, animals were injected IP with 150 mg/kg D-Luciferin (PerkinElmer) and anesthetized using 3% isoflurane and transferred to the chamber of an IVIS Lumina XR (PerkinElmer), where they received 2% isoflurane throughout image acquisition. Analysis was performed using Living Image software, v4.3.

Processing of animal tissues, fluorescence microscopy and morphometric analysis of animal metastases

Bones and soft tissue organs were harvested and processed, and fluorescent images of DTCs and tumor foci obtained as previously described [5,25]. Tumor area measurements were conducted using the Nuance Software (v. 2.4) and calibration with a TS-M2 stage micrometer (Oplenic Optronics). Statistical analysis between groups used either unpaired, two-tailed Student's *t*-test or one-way Anova test.

Immunohistochemistry and analysis of human bone metastases

De-identified FFPE biopsy specimens of bone metastatic lesions from two different cohorts of advanced prostate cancer patients were obtained from the archives of the Departments of Pathology at Drexel University College of Medicine (5 patients) and at Thomas Jefferson University (5 patients), and stained using the aforementioned antibody against the N-20 region of the human Androgen Receptor, or against Prostein (Clone 10E3). These biopsy specimens were used to determine AR expression in cancer cells across 57 distinct regions of interest. Two board-certified pathologists (F.U.G and Y.G) selected the tumor areas to be inspected for AR expression by examining paired serial sections stained with Hematoxylin/Eosin. Assessment of AR staining intensity was performed using the Aperio system and ImageScope software (Leica).

Laser Capture Microdissection

For Laser Capture Microdissection (LCM) mouse tissues were prepared and frozen in OCT compound and cut to 40-μm sections. Tissue slides were washed with ice-cold RNase-free water for 2 minutes then immediately dehydrated using an ethanol gradient in order to maintain RNA integrity.

For four human specimens, human FFPE sections subsequent to those used for IHC were deparaffinized in ice-cold xylene substitute for 15 minutes and dehydrated in ethanol for 30

seconds. LCM was performed using a PALM MicroBeam system (Zeiss). Microdissected tissues were catapulted into Zeiss AdhesiveCap 200 tubes and stored at −80 °C until RNA extraction.

qRT-PCR

Microdissected tissue samples were slowly thawed at room temperature, followed by RNA extraction using the RNeasy FFPE Kit (Qiagen). Human RNA samples were amplified using the Ovation Pico WTA system V2 (NuGEN). Extracted mouse RNA samples and amplified human cDNA samples were stored at −80 °C until qRT-PCR was performed using an Applied Biosystems 7900HT Fast Real-Time PCR System. Gene-specific primer-probe sets were purchased from Applied Biosystems/Life Technologies (Supplemental table 2).

Nanostring Profiling

We used 100ng of total RNA (20ng/μl) on the nCounter Pan Cancer immune profiling for mouse, which includes 750 genes with established relevance in immune response plus 40 housekeeping genes used for normalization and selected with a geNorm algorithm. The nSolver (v.2.5) user interface was used to operate the nCounter Advanced analysis module, which employs the R statistical software.

Supplementary Material

Refer to Web version on PubMed Central for supplementary material.

Acknowledgments

This work was supported by NIH F30CA192896-01 grant to K.S. and in part by Department of Defense PC080987 Idea Award to A.F. We thank Dr. Olimpia Meucci (Department of Pharmacology and Physiology at Drexel University College of Medicine) for invaluable advice, Dr. Kevin Kelly (Medical Oncology) and all the other members of the Greater Philadelphia Prostate Cancer Working Group at the Sidney Kimmel Cancer Center, Thomas Jefferson University for insightful discussions, Dr. Ruth Birbe (Pathology) at Thomas Jefferson University for providing the human specimens of skeletal metastases and Danielle Jernigan (Fatatis lab) for critical reading of the manuscript.

References

1. Voronov E, Shouval DS, Krelin Y, Cagnano E, Benharroch D, Iwakura Y, et al. IL-1 is required for tumor invasiveness and angiogenesis. Proc Natl Acad Sci USA. 2003; 100:2645–2650. [PubMed: 12598651]
2. Lewis AM, Varghese S, Xu H, Alexander HR. Interleukin-1 and cancer progression: the emerging role of interleukin-1 receptor antagonist as a novel therapeutic agent in cancer treatment. J Transl Med. 2006; 4:48. [PubMed: 17096856]
3. Valdivia-Silva JE, Franco-Barraza J, Silva ALE, Pont GD, Soldevila G, Meza I, et al. Effect of pro-inflammatory cytokine stimulation on human breast cancer: implications of chemokine receptor expression in cancer metastasis. Cancer Letters. 2009; 283:176–185. [PubMed: 19409696]
4. Dinarello CA. Why not treat human cancer with interleukin-1 blockade? Cancer Metastasis Rev. 2010; 29:317–329. [PubMed: 20422276]
5. Liu Q, Russell MR, Shahriari K, Jernigan DL, Lioni MI, Garcia FU, et al. Interleukin-1β promotes skeletal colonization and progression of metastatic prostate cancer cells with neuroendocrine features. Cancer Res. 2013; 73:3297–3305. [PubMed: 23536554]
6. Eckhardt BL. Strategies for the discovery and development of therapies for metastatic breast cancer. Nature reviews Drug discovery. 2012; 11:479–497. [PubMed: 22653217]

7. Wang M, Stearns ME. Isolation and characterization of PC-3 human prostatic tumor sublines which preferentially metastasize to select organs in S.C.I.D. mice. Differentiation. 1991; 48:115–125. [PubMed: 1773917]
8. Russell MR, Jamieson WL, Dolloff NG, Fatatis A. The alpha-receptor for platelet-derived growth factor as a target for antibody-mediated inhibition of skeletal metastases from prostate cancer cells. Oncogene. 2009; 28:412–421. [PubMed: 18850002]
9. Dinarello CA, Simon A, van der Meer JWM. Treating inflammation by blocking interleukin-1 in a broad spectrum of diseases. Nature reviews Drug discovery. 2012; 11:633–652. [PubMed: 22850787]
10. Madar S, Goldstein I, Rotter V. 'Cancer associated fibroblasts' – more than meets the eye. Trends Mol Med. 2013; 19:447–453. [PubMed: 23769623]
11. Orimo A, Gupta PB, Sgroi DC, Arenzana-Seisdedos F, Delaunay T, Naeem R, et al. Stromal fibroblasts present in invasive human breast carcinomas promote tumor growth and angiogenesis through elevated SDF-1/CXCL12 secretion. Cell. 2005; 121:335–348. [PubMed: 15882617]
12. Giannoni E, Bianchini F, Masieri L, Serni S, Torre E, Calorini L, et al. Reciprocal activation of prostate cancer cells and cancer-associated fibroblasts stimulates epithelial-mesenchymal transition and cancer stemness. Cancer Res. 2010; 70:6945–6956. [PubMed: 20699369]
13. Karagiannis GS, Poutahidis T, Erdman SE, Kirsch R, Riddell RH, Diamandis EP. Cancer-associated fibroblasts drive the progression of metastasis through both paracrine and mechanical pressure on cancer tissue. Mol Cancer Res. 2012; 10:1403–1418. [PubMed: 23024188]
14. Li H-J, Reinhardt F, Herschman HR, Weinberg RA. Cancer-Stimulated Mesenchymal Stem Cells Create a Carcinoma Stem Cell Niche via Prostaglandin E2 Signaling. Cancer Discovery. 2012; 2:840–855. [PubMed: 22763855]
15. Garrett SC, Varney KM, Weber DJ, Bresnick AR. S100A4, a Mediator of Metastasis. J Biol Chem.
16. Weckermann D, Müller P, Wawroschek F, Harzmann R, Riethmüller G, Schlimok G. Disseminated cytokeratin positive tumor cells in the bone marrow of patients with prostate cancer: detection and prognostic value. J Urol. 2001; 166:699–703. [PubMed: 11458120]
17. Xu J, Kalos M, Stolk JA, Zasloff EJ, Zhang X, Houghton RL, et al. Identification and characterization of prostein, a novel prostate-specific protein. Cancer Res. 2001; 61:1563–1568. [PubMed: 11245466]
18. Kalos M, Askaa J, Hylander BL, Repasky EA, Cai F, Vedvick T, et al. Prostein expression is highly restricted to normal and malignant prostate tissues. Prostate. 2004; 60:246–256. [PubMed: 15176054]
19. Sheridan T, Herawi M, Epstein JI, Illei PB. The role of P501S and PSA in the diagnosis of metastatic adenocarcinoma of the prostate. The American Journal of Surgical Pathology. 2007; 31:1351–1355. [PubMed: 17721190]
20. Cindolo L, Franco R, Cantile M, Schiavo G, Liguori G, Chiodini P, et al. NeuroD1 expression in human prostate cancer: can it contribute to neuroendocrine differentiation comprehension? European Urology. 2007; 52:1365–1373. [PubMed: 17126478]
21. Komiya A, Suzuki H, Imamoto T, Kamiya N, Nihei N, Naya Y, et al. Neuroendocrine differentiation in the progression of prostate cancer. Int J Urol. 2009; 16:37–44. [PubMed: 19120524]
22. Bersani F, Lee J, Yu M, Morris R, Desai R, Ramaswamy S, et al. Bioengineered implantable scaffolds as a tool to study stromal-derived factors in metastatic cancer models. Cancer Res. 2014; 74:7229–7238. [PubMed: 25339351]
23. Drake JM, Gabriel CL, Henry MD. Assessing tumor growth and distribution in a model of prostate cancer metastasis using bioluminescence imaging. Clin Exp Metastasis. 2005; 22:674–684. [PubMed: 16703413]
24. Drake JM, Danke JR, Henry MD. Bone-specific growth inhibition of prostate cancer metastasis by atrasentan. Cancer Biol Ther. 2010; 9:607–614. [PubMed: 20139704]
25. Shen F, Zhang Y, Jernigan DL, Feng X, Yan J, Garcia FU, et al. Novel Small-Molecule CX3CR1 Antagonist Impairs Metastatic Seeding and Colonization of Breast Cancer Cells. Mol Cancer Res. 2016; 14:518–527. [PubMed: 27001765]

26. Cohen SB. The use of anakinra, an interleukin-1 receptor antagonist, in the treatment of rheumatoid arthritis. Rheum Dis Clin North Am. 2004; 30:365–80. vii. [PubMed: 15172046]
27. Boye K, Mælandsmo GM. S100A4 and Metastasis. Am J Pathol. 2010; 176:528–535. [PubMed: 20019188]
28. Goel HL, Li J, Kogan S, Languino LR. Integrins in prostate cancer progression. Endocr Relat Cancer. 2008; 15:657–664. [PubMed: 18524948]
29. Hemingway F, Taylor R, Knowles HJ, Athanasou NA. RANKL-independent human osteoclast formation with APRIL, BAFF, NGF, IGF I and IGF II. Bone. 2011; 48:938–944. [PubMed: 21193069]
30. Wai PY, Kuo PC. Osteopontin: regulation in tumor metastasis. Cancer Metastasis Rev. 2008; 27:103–118. [PubMed: 18049863]
31. Yu D, Zhong Y, Li X, Li Y, Li X, Cao J, et al. ILs-3, 6 and 11 increase, but ILs-10 and 24 decrease stemness of human prostate cancer cells in vitro. Oncotarget. 2015; 6:42687–42703. [PubMed: 26528857]
32. Pio R, Corrales L, Lambris JD. The role of complement in tumor growth. Adv Exp Med Biol. 2014; 772:229–262. [PubMed: 24272362]
33. Kim S, Iizuka K, Aguila HL, Weissman IL, Yokoyama WM. In vivo natural killer cell activities revealed by natural killer cell-deficient mice. Proc Natl Acad Sci USA. 2000; 97:2731–2736. [PubMed: 10694580]
34. Therapeutic approaches to enhance natural killer cell cytotoxicity against cancer: the force awakens. 2015; 14:487–498.
35. Shariff AH, Ather MH. Neuroendocrine differentiation in prostate cancer. Urology. 2006; 68:2–8.
36. Jiborn T, Bjartell A, Abrahamsson PA. Neuroendocrine differentiation in prostatic carcinoma during hormonal treatment. Urology. 1998; 51:585–589. [PubMed: 9586611]
37. Sun Y, Niu J, Huang J. Neuroendocrine differentiation in prostate cancer. Am J Transl Res. 2009; 1:148–162. [PubMed: 19956427]
38. Beltran H, Rickman DS, Park K, Chae SS, Sboner A, MacDonald TY, et al. Molecular Characterization of Neuroendocrine Prostate Cancer and Identification of New Drug Targets. Cancer Discovery. 2011; 1:487–495. [PubMed: 22389870]
39. Sharma A, Yeow W-S, Ertel A, Coleman I, Clegg N, Thangavel C, et al. The retinoblastoma tumor suppressor controls androgen signaling and human prostate cancer progression. J Clin Invest. 2010; 120:4478–4492. [PubMed: 21099110]
40. Zhao Y, Tindall DJ, Huang H. Modulation of androgen receptor by FOXA1 and FOXO1 factors in prostate cancer. Int J Biol Sci. 2014; 10:614–619. [PubMed: 24948874]
41. Fenton MJ. Review: transcriptional and post-transcriptional regulation of interleukin 1 gene expression. Int J Immunopharmacol. 1992; 14:401–411. [PubMed: 1618594]
42. Klein CA. Selection and adaptation during metastatic cancer progression. Nature. 2013; 501:365–372. [PubMed: 24048069]
43. Bedard PL, Hansen AR, Ratain MJ, Siu LL. Tumour heterogeneity in the clinic. Nature. 2013; 501:355–364. [PubMed: 24048068]
44. Mickey DD, Stone KR, Wunderli H, Mickey GH, Vollmer RT, Paulson DF. Heterotransplantation of a human prostatic adenocarcinoma cell line in nude mice. Cancer Res. 1977; 37:4049–4058. [PubMed: 908039]
45. Tabassum DP, Polyak K. Tumorigenesis: it takes a village. Nat Rev Cancer. 2015; 15:473–483. [PubMed: 26156638]
46. Wurth R, Tarn K, Jernigan D, Fernandez SV, Cristofanilli M, Fatatis A, et al. A Preclinical Model of Inflammatory Breast Cancer to Study the Involvement of CXCR4 and ACKR3 in the Metastatic Process. Transl Oncol. 2015; 8:358–367. [PubMed: 26500026]
47. Jamieson-Gladney WL, Zhang Y, Fong AM, Meucci O, Fatatis A. The chemokine receptor CX3CR1 is directly involved in the arrest of breast cancer cells to the skeleton. Breast Cancer Research. 2010; 12:307. [PubMed: 20727231] 2011; 13:R91.

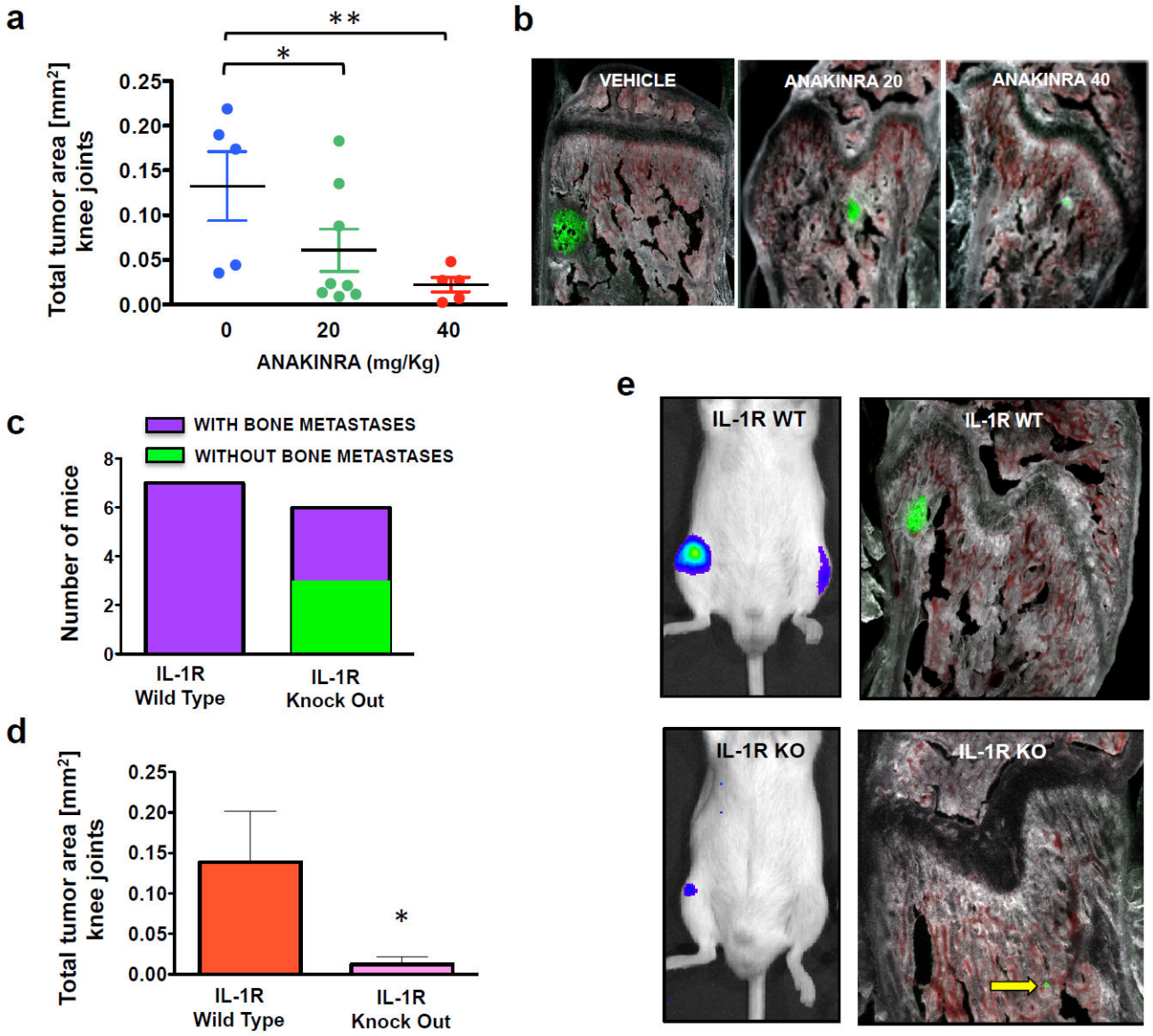

Figure 1. Targeting IL-1β in animal models and evidence that tumor-derived IL-1β recruits the bone stroma in the metastatic niche

(**a, b**) Animals were treated daily with the IL-1R antagonist anakinra or vehicle starting one day prior to cancer cell inoculation and continuing until sacrifice at two weeks. Total tumor area measured in both knee joints for each mouse showed a dose-dependent reduction in response to anakinra treatment; at the higher dose, the decrease in tumor burden was comparable to that observed in our previous studies using shRNA-mediated IL-1β knockdown in PC3-ML cells [5]. Five animals each were used for vehicle and 40mg/Kg anakinra, eight animals 20mg/Kg anakinra. (**c**) SCID mice wild-type (WT) or null (KO) for the IL-1R inoculated with PC3-ML cells and sacrificed after two weeks. Upon sacrifice, 50% of the knockout animals were free of metastatic lesions in the knee joint, while all wild-type animals harbored tumors. (**d, e**) Among the IL-1R KO mice that did form tumors, total

tumor area was significantly reduced relative to their WT counterparts. Seven animals were used for IL-1R WT and six animals for IL-1R KO. (Dot-plot data: *p= 0.03; **p=0.008 by One-way ANOVA – Total tumor area data are expressed as mean ± S.E. *p<0.05 by Student's t-test).

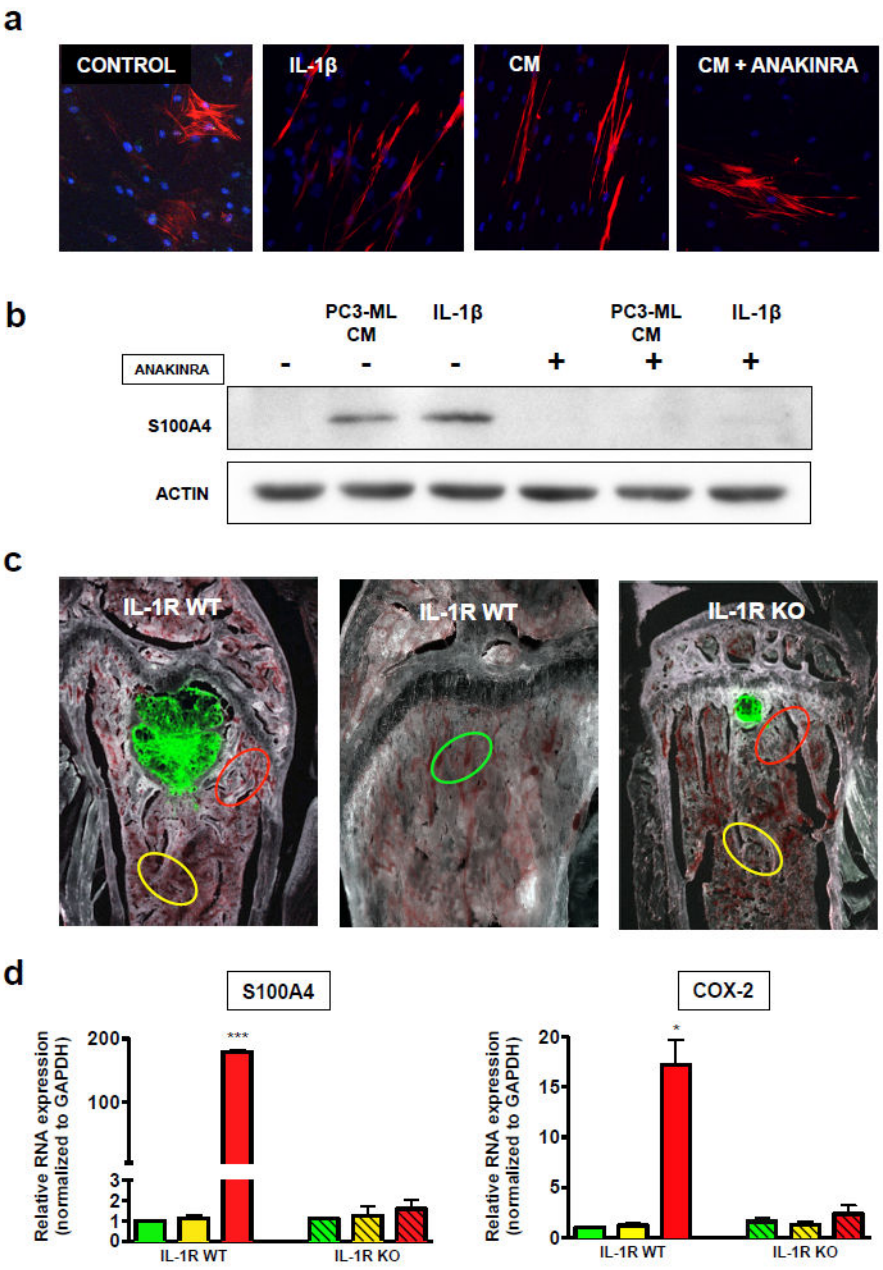

Figure 2. IL-1β converts hMSC into CAFs *in vitro* and induces carcinoma-associated phenotypes *in vivo*

(**a**) hMSCs were treated for one week with regular medium, recombinant human IL-1β peptide (25 pg/mL) or CM from PC3-ML cells with and without anakinra (10 μg/mL). Cells were then stained for α-smooth muscle actin (red) and DAPI (blue), revealing linear stress fibers in response to both IL-1β and PC3-ML CM, which were abrogated by the inclusion of anakinra. (**b**) hMSCs treated as above were lysed and subjected to western blotting for actin and the CAF marker S100A4, which was up-regulated in response to IL-1β and PC3- ML CM, an effect fully abolished in the presence of anakinra. (**c**) SCID mice wild-type (WT) and null (KO) for IL-1R were inoculated with fluorescently-labeled PC3-ML human

prostate cancer cells and sacrificed after three weeks; LCM was used to harvest bone stromal regions adjacent to tumors (red), distant from tumors (yellow), and from tumor-free bones (green). (**d**) upon qRT-PCR analysis of these samples, S100A4 was found to be specifically up-regulated exclusively in the tumor-associated stroma of WT animals, indicating a local effect dependent on IL-1β signaling. Similarly, the IL-1β downstream target COX-2 was up regulated only in WT tumor-associated stroma. Samples from three animals of each genotype were analyzed. (Data are expressed as mean ± S.E; ***p=0.0002; *p=0.002 by one-way ANOVA with Tukey post-test).

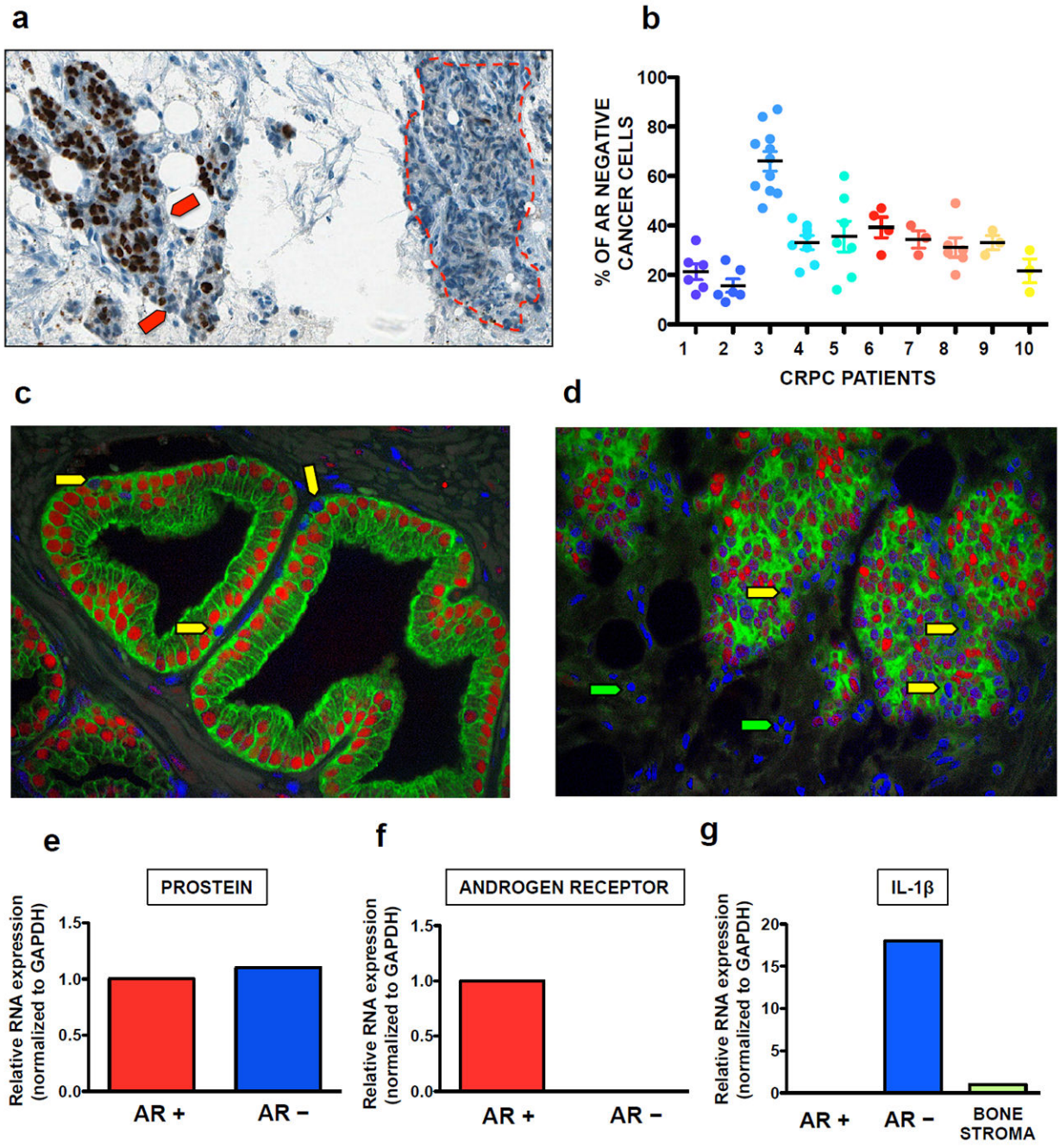

Figure 3. AR and IL-1β expression in human skeletal metastases

(**a**) Cancer cells lacking nuclear AR staining (red arrows) were commonly detected intermixed with AR+ cells and frequently comprised the vast majority of large foci (red dotted line). (**b**) The fraction of cancer cells negative for AR expression detected in bone metastases from ten CRPC patients was found to be 33±14%, with the percentage of infiltrating or resident non-cancerous cells (immune, endothelial or stromal origin) not exceeding 1-2%. (**c, d**) Primary tumor (**c**) and bone metastatic (**d**) tissues were stained with both a pan-cytokeratin antibody (green) and the AR antibody used in A-D (red), with nuclei

in blue. Both AR+ (red nuclei) and AR− (blue nuclei) cancer cells are of epithelial origin and are present in the basal compartment of primary tumors as well as mixed with AR+ cells in skeletal metastases (yellow arrows). Non-epithelial AR− cells were identified in the bone marrow stroma (green arrows). (**e, g**) Bone metastasis specimens from four of the same CRPC patients previously tested for AR expression by IHC were selected for LCM-mediated harvesting of tumor areas negative or positive for AR as well as normal stromal tissue. (**e**) qRT-PCR detected the prostate-specific marker prostein expressed at comparable levels in prostate cancer cells independently of their AR status. (**f**) The lack of AR expression in cells that stained negative by immunohistochemistry was confirmed at the transcriptional level. (**g**) IL-1β mRNA was detected exclusively in AR− cancer cells, while considerably lower levels of this cytokine were detected in the bone stroma.

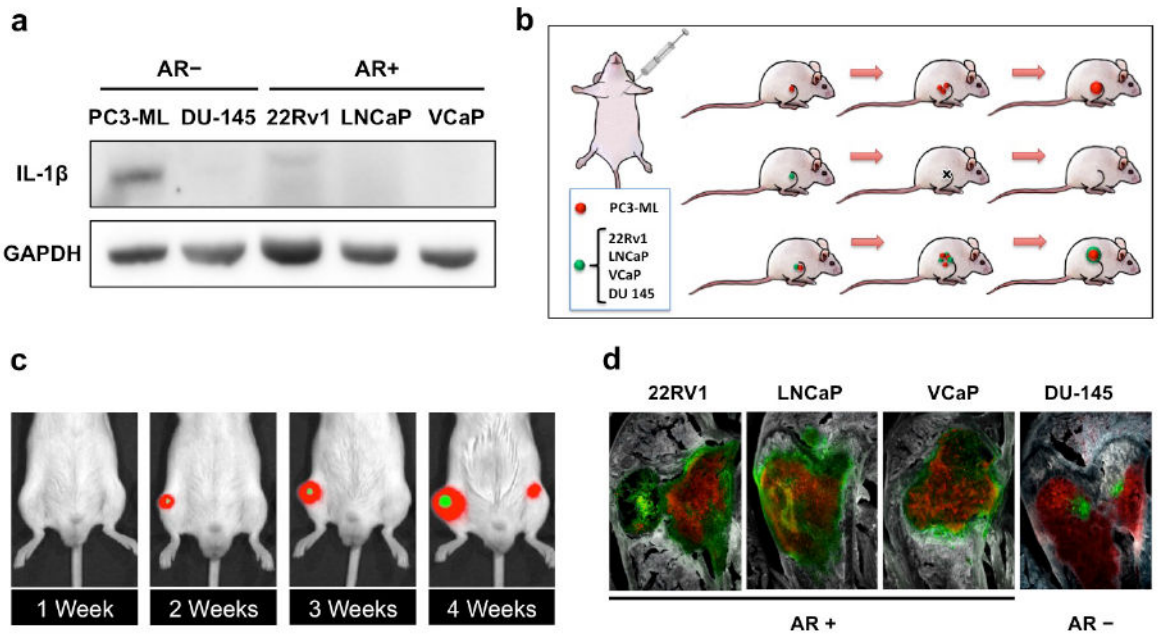

Figure 4. Cancer cell cooperation in the bone metastatic niche

(**a**) PC3-ML cells express IL- 1β protein, in contrast to all other human prostate cancer cell lines tested. (**b**) Schematic of experimental design: Highly bone-metastatic PC3-ML cells were engineered to stably express both the mCherry red-fluorescent protein and Red Firefly Luciferase (RedLuc). Non-metastatic 22Rv1, LNCaP, VCaP and DU-145 were engineered to stably expressing GFP and Luc2 luciferase. (**c**) When co-inoculated with PC3-ML cells, each of the independently non-metastatic cancer cell lines generated bone tumors, detected by both bioluminescence *in vivo* imaging (**c**) and multispectral fluorescence microscopy (**d**). The relative fractions of mixed tumors for each non-metastatic cell type were as follows: 59% for LNCaP (9 mice), 78% VCaP (9 mice), 59% 22Rv1(13 mice) and 93% for DU-145 (4 mice).

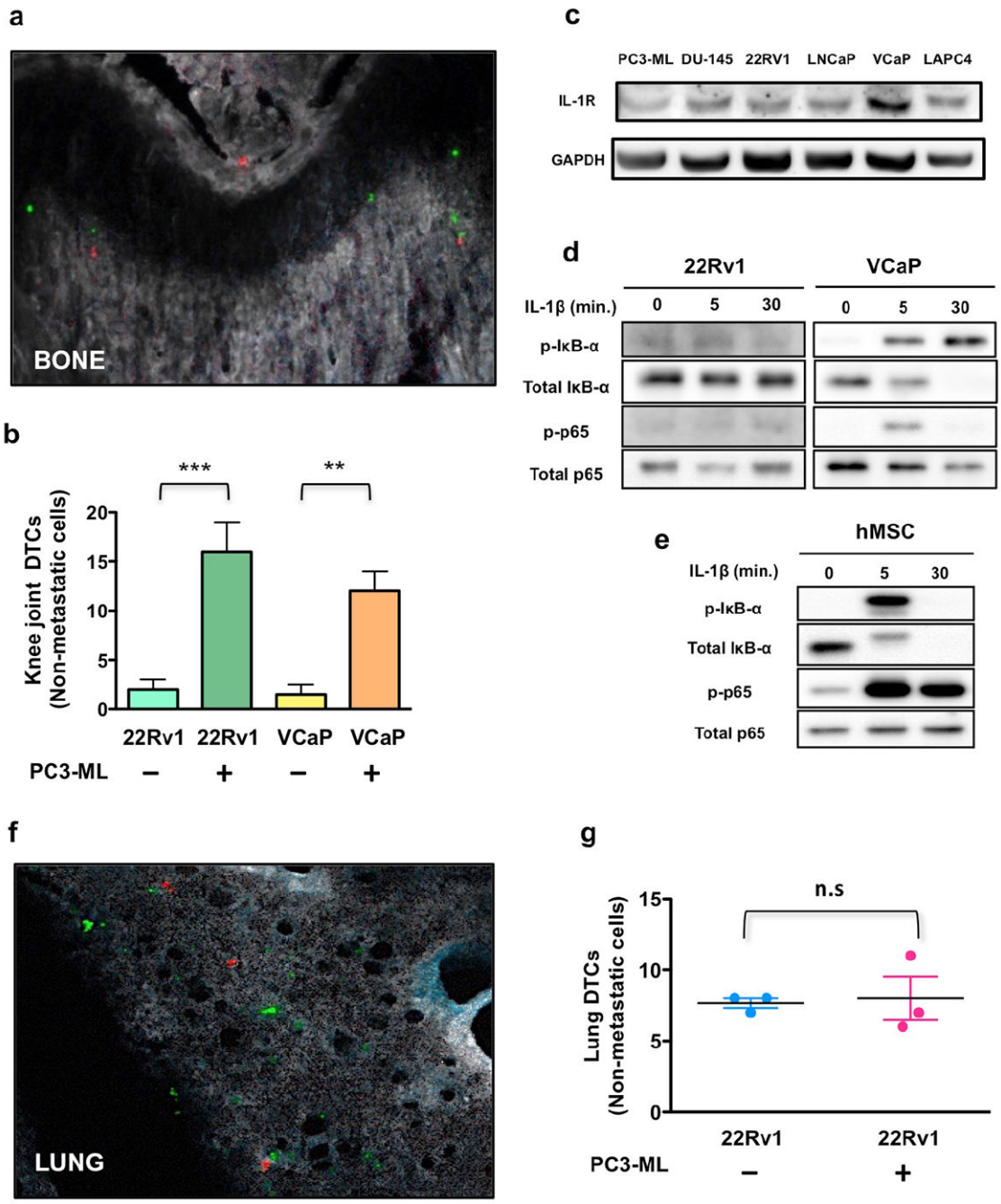

Figure 5. Cooperation between metastatic and non-metastatic prostate cancer cells is an early event

Co-inoculation with PC3-ML cells dramatically increased the number of 22Rv1 or VCaP that lodged to the bone (**a,b**) when compared to either of these cell types inoculated alone. All AR− and AR+ prostate cancer cells examined express IL-1R (**c**). However, 22Rv1 and VCaP cells showed diverging signaling in response to exogenous treatment with IL-1β (**d**), whereas hMSC responded to the cytokine with a strong activation of the NF-kB pathway (**e**). In lungs the number of 22Rv1 cells detected 24 hours post-inoculation was independent of

co-inoculation of PC3-ML cells (**f,g**). Results are shown as mean ± S.E; 3 animals for each group. ** p=0.01, and *** p=0.006 by Student's t-test. Magnification: 200x

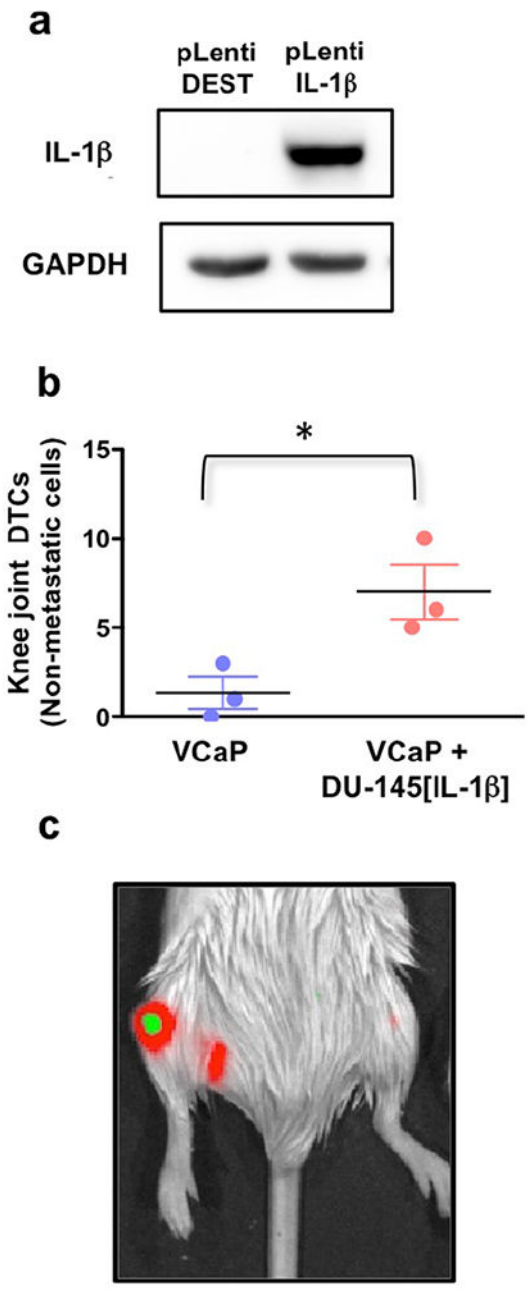

Figure 6. Exogenous expression of IL-1β confers a pro-metastatic supportive role to PCa cells

DU-145 cells engineered to over-express IL-1β (**a**) and co-inoculated with VCaP cells replicated the supportive effect provided by PC3-ML cells (**b**). Results are shown as mean ± S.E; 3 animals for each group. *$p = 0.03$ by Student's *t*-test.

Table 1

Genes either up-regulated or down-regulated by at least 2 folds in tumor-associated bone stroma

Genes showing alteration by 3 folds or more are labeled with darker color hues.

GENE NAME	ACCESSION NUMBER	FOLD CHANGE	p VALUE	
Abcb1a	NM_011076.1	4.82	0.0026	Multidrug resistance protein 1
Angpt1	NM_009640.3	3.66	0.01	Angiopoietin
Ccl5	NM_013653.3	3.53	0.0375	Chemokine
Itgb2	NM_008404.4	3.25	0.0093	Integrin beta 2
Ptgs2	NM_011198.3	3.21	0.0058	COX-2
Cfh	NM_009888.3	2.89	0.0299	Regulator of complement activation
Spp1	NM_009263.3	2.81	0.0049	Osteopontin
Birc5	NM_009689.2	2.72	0.0405	IAP member
Itga1	NM_001033228.3	2.69	0.0186	Integrin alpha 1
Tnfrsf17	NM_011608.1	2.62	0.039	TNF receptor – binds TNF13b
Fos	NM_010234.2	2.43	0.0432	Oncogene
Vim	NM_011701.4	2.28	0.0211	Vimentin
Tnfsf13b	NM_033622.1	2.17	0.0085	TNF13b
Itgb4	NM_001005608.2	2.16	0.0449	Integrin beta 4
Dusp6	NM_026268.2	2.01	0.0085	Dual specific phosphatase 6
H2-Dma	NM_010386.3	-2	0.0125	Histocompatibility 2, class II, locus DMa
Ecsit	NM_001253897.1	-2.06	0.0488	Signaling integrator
Thbs1	NM_011580.3	-2.16	0.0362	Trombospondin 1
Cxcl5	NM_009141.2	-2.17	0.0135	Chemokine
Mcam	NM_023061.2	-2.37	0.0195	Melanoma cell adhesion molecule
Cd34	NM_001111059.1	-2.39	0.0068	Cell surface glycoprotein
Trp53	NM_011640.1	-2.5	0.018	Tumor suppressor
C1ra	NM_023143.3	-2.51	0.0205	Complement component 1r
Tfeb	NM_001161723.1	-3.08	0.0046	Transcription factor EB
Masp2	NM_010767.3	-3.21	0.0357	Mannan-binding Lectin Serine Peptidase 2
Cdh1	NM_009864.2	-3.3	0.0326	Cadherin 1
Hspb2	NM_024441.3	-3.44	0.0132	Heat shock protein 2
Cd74	NM_001042605.1	-4.01	0.0249	Major histocompatibility complex, class II
C1s1	NM_144938.2	-6.09	0.0095	Complement component 1, subcomp. 1
Il24	NM_053095.2	-6.86	0.0165	Interleukin 24